Anal. Chem. **2002,** *74,* 2048−2052

Thermal Vaporization-Vacuum Ultraviolet Laser Ionization Time-of-Flight Mass Spectrometry of Single Aerosol Particles

D. Craig Sykes, Ephraim Woods, III, Geoffrey D. Smith, Tomas Baer,* and Roger E. Miller

Department of Chemistry, University of North Carolina, Chapel Hill, North Carolina 27599-3290

Single aerosol particles of ethylene glycol and oleic acid are vaporized on a heater at temperatures between 500 and 700 K, and the resulting vapor plume is ionized by a 10.5-eV vacuum ultraviolet (VUV) laser. The mass spectra are compared to those obtained by CO_2 laser vaporization followed by VUV laser ionization. The relative intensities of the parent and fragment ion peaks are remarkably similar for the two modes of vaporization. A Maxwell−Boltzmann distribution of speeds accurately describes the dependence of the signal as a function of the VUV laser pulse timing. The signal levels obtained with this design are sufficient to obtain good-quality mass spectra.

An important milestone in the chemical analysis of aerosols is the development of laser desorption/ionization mass spectrometric methods capable of determining the chemical composition of single aerosol particles in real time. The first demonstration of single aerosol particle analysis employed a Nd:YAG (266 nm) laser pulse for desorption/ionization of the particles, followed by ion analysis with a quadrupole mass spectrometer.[1] Although this technique provided the first single-particle analysis, the use of a quadrupole mass spectrometer did not allow for characterization of the entire particle since this analyzer monitors only one ion mass at a time. The real power of the technique was achieved by linking the laser desorption/ionization with time-of-flight (TOF) mass spectrometry,[2] which yielded a complete mass spectrum for a single particle. Among the lasers used for this purpose have been the 266-nm output from a Nd:YAG laser, and the 193-, 248-, and 308-nm excimer lasers.[3−5] Although this method works very well for inorganic aerosol constituents (salts), a major limitation associated with the use of a single laser to both vaporize and ionize is the high power required for this process and the resulting fragmentation of the more delicate organic ions in the laser field. As a result, such instruments can detect the presence of organic species but, in general, are not capable of identifying them.

In response to this problem, a two-step method of desorption/ionization was developed[6−8] in which a CO_2 laser (10.6 μm) vaporizes aerosol particles prior to multiphoton ionization using frequency-quadrupled Nd:YAG lasers (266 nm)[6] and ArF excimer lasers(193 nm).[8] The major advantages of this two-step method lie in the ability to use lower ionization laser power densities and to adjust the vaporization and ionization lasers individually. However, the use of multiphoton ionization with UV lasers still caused many organic ions to fragment excessively in the high laser field. More recently, vacuum ultraviolet (VUV) light has been used for the ionization process,[9] in which a single photon gently ionizes the molecules and produces primarily parent ions with little fragmentation.

While IR/VUV laser mass spectrometry is well-suited for laboratory environments, it is not practical for portable field instruments that analyze aerosols in ground and aircraft environments. The physical size of the CO_2 laser is the major problem in adapting the two-laser vaporization/ionization scheme to portable single-particle instruments. An alternative method is thermal vaporization on a hot filament, an approach that dates back to the early 1980s[10,11] and has been recently employed by several groups in combination with electron impact ionization (EI) of the vaporized particle.[12−14] This technique has proven to be practical for characterizing particles that are too small for detection by most current single-particle mass spectrometers, while permitting the analysis of organic species by the well-known EI method for which copious reference spectra are available for product identification. However, these quadrupole ionization instruments are also incapable of recording a complete mass spectrum for a single particle, unless coupled with a space charge potential well that

(1) Sinha, M. P. *Rev. Sci. Instrum.* **1984**, *55*, 886−891.
(2) McKeown, P. J.; Johnston, M. V.; Murphy, D. M. *Anal. Chem.* **1991**, *63*, 2069−2073.
(3) Carson, P. G.; Neubauer, K. R.; Johnston, M. V.; Wexler, A. S. *J. Aerosol Sci.* **1995**, *26*, 535−545.
(4) Murphy, D. M.; Thomson, D. S. *Aerosol Sci. Technol.* **1995**, *22*, 237−249.
(5) Silva, P. J.; Prather, K. A. *Anal. Chem.* **2000**, *72*, 3553−3562.
(6) Morrical, B. D.; Fergenson, D. P.; Prather, K. A. *J. Am. Soc. Mass Spectrom.* **1998**, *9*, 1068−1073.
(7) Zelenyuk, A.; Cabalo, J.; Baer, T.; Miller, R. E. *Anal. Chem.* **1999**, *71*, 1802−1808.
(8) Cabalo, J.; Zelenyuk, A.; Baer, T.; Miller, R. E. *Aerosol Sci. Technol.* **2000**, *33*, 3−19.
(9) Woods, E., III; Smith, G. D.; Dessiaterik, Y.; Baer, T.; Miller, R. E. *Anal. Chem.* **2001,** *73*, 2317−2322.
(10) Allen, J.; Gould, R. K. *Rev. Sci. Instrum.* **1981**, *52*, 804−809.
(11) Sinha, M. P.; Giffin, C. E.; Norris, D. D.; Estes, T. J.; Vilker, V. L.; Friedlander, S. K. *J. Colloid Interface Sci.* **1982**, *87*, 140−153.
(12) Tobias, H. J.; Kooiman, P. M.; Docherty K. S.; Ziemann, P. J. *Aerosol Sci. Technol.* **2000**, *33*, 170−190.
(13) Jayne, J. T.; Leard, D. C.; Zhang, X.; Davidovits, P.; Smith, K. A.; Kolb, C. E.; Worsnop, D. R. *Aerosol Sci. Technol.* **2000**, *33*, 49−70.
(14) Coggiola, M. J.; Shi, Z.; Young, S. E. *Aerosol Sci. Technol.* **2000**, *33*, 20−29.

10.1021/ac011225a CCC: $22.00
Published on Web 03/26/2002

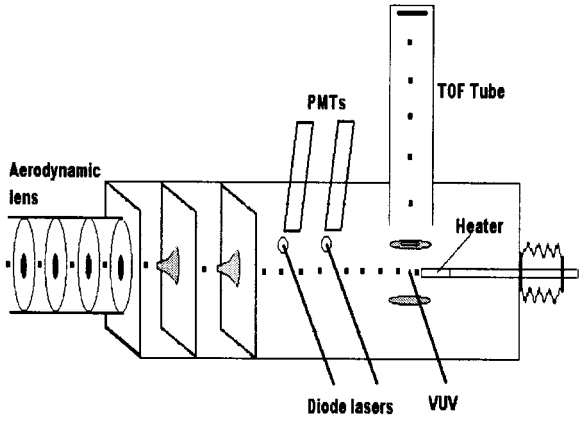

Figure 1. Diagram of the single aerosol particle mass spectrometer. Aerosol particles are introduced into the aerodynamic lens and accelerated by a supersonic gas expansion. Size-selected particles then hit the heater where they are vaporized. The resulting vapor plume is ionized by a vacuum ultraviolet laser pulse and the ions mass analyzed by their time of flight.

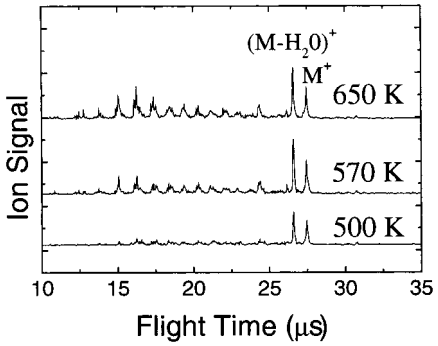

Figure 2. TOF mass spectra of oleic acid at three heater temperatures. The spectrum is the average of 100 single-particle mass spectra. The increased fragmentation at the higher energies is the result of higher internal energy of the vapor plume.

stores the ions for later extraction and analysis by TOF, as is done by Coggiola et al.[14]

In this paper, we combine thermal vaporization with VUV photoionization to assemble a simple but robust single aerosol particle mass spectrometer that is suitable for detecting organic molecules. The major advantage of VUV photoionization over EI is the reduced fragmentation of the organic ions, a property that will be useful for analyzing complex mixtures. The technical challenges are the optimization of the overlap between the laser beam and the slowly expanding vapor plume from a single particle, and the efficient extraction of the ions into the TOF mass spectrometer.

EXPERIMENTAL APPROACH

The instrument used for the two-step laser desorption/ionization was described in detail in previous publications.[8,9] The only changes required to convert this instrument into one capable of thermal vaporization studies were the insertion of a cartridge heater between the extraction plates of the time-of-flight mass spectrometer and the adjustment of the timing circuitry for the firing of the VUV ionization laser. Figure 1 shows the arrangement of the main components of the instrument. Thermal vaporization on the hot filament was tested with oleic acid (9-octadecenoic acid) and ethylene glycol (1,2-ethanediol) particles. The oleic acid was generated from dilute solutions in methyl alcohol by either a glass nebulizer (Meinhard) or by a vibrating orifice aerosol generator (VOAG; TSI model 3450). The ethylene glycol particles were nebulized without dilution.

The particles are focused into a narrowly collimated beam by an aerodynamic lens system as described by Liu et al.[15,16] The supersonic expansion at the outlet of the aerodynamic lens accelerates each particle to a terminal velocity that is proportional to its aerodynamic diameter. The particles enter the main chamber where they pass through two 532-nm green diode laser beams separated by 10 cm. The scattered light generated as the particles pass through the two continuous wave laser beams is detected by separate PMTs. The delay between these light-scattering signals determines the particle's velocity (and thus, its size). Signals from the photomultipliers are also used to trigger the pulsed vaporization or ionization lasers when the particle reaches the ionization region of the TOF-MS. In the case of the two-step laser desorption/ionization experiment, a pulsed TEA−CO_2 laser (Lumonics) producing 10.6-μm radiation is focused to a spot size of ~1 mm^2 and is used to vaporize the particle. After the vapor plume is formed, a pulse of 118-nm VUV light, produced by tripling the 355-nm light from a Nd:YAG laser (Continuum), is used to ionize the gas-phase molecules. The VUV laser is also focused to about a 1-mm^2 spot, but its center is displaced by ~0.25 mm to take into account the distance traveled by the vapor plume in the 2−10-μs delay between the firing of the IR and VUV lasers.

For the thermal vaporization experiment, a 6.5-mm-diameter cartridge heater (Watlow Electric) was substituted for the CO_2 laser. The heater, which contained an internal thermocouple, was mounted on a 6.5-mm-diameter stainless steel rod for insertion into the chamber. A translation stage was constructed to allow for *x*, *y*, *z* alignment of the heater with respect to the particle beam. The heater was located between the ion extraction plates, about 8−10 mm beyond the ionization region. Particle vaporization occurred upon contact with the heater surface, and the resulting vapor plume was then ionized by a pulse of VUV light. After ionization, the ions were accelerated into a 1-m field-free region of a time-of-flight mass spectrometer, where the ion signal was detected by a set of multichannel plates (MCPs). This signal was then digitized by a digital oscilloscope (HP, Infinium) and transferred to a computer through a GPIB connection. Although single-particle mass spectra were generated, all spectra presented in this paper were obtained by averaging the signals from 100 particles.

RESULTS AND DISCUSSION

Evidence of Single-Particle Analysis. Figure 2 shows typical mass spectra of vaporized oleic acid particles in a range of sizes from 2 to 4 μm obtained by impinging the particles on the heater and ionizing the resulting vapor with the VUV laser. However, before discussing these results, we need to establish that they originate from photoionization of single particles and not simply

(15) Liu, P.; Ziemann, P. J.; Kittelson, D. B.; McMurry, P. H. *Aerosol Sci. Technol.* **1995**, *22*, 293−313.
(16) Liu, P.; Ziemann, P. J.; Kittelson, D. B.; McMurry, P. H. *Aerosol Sci. Technol.* **1995**, *22*, 314−324.

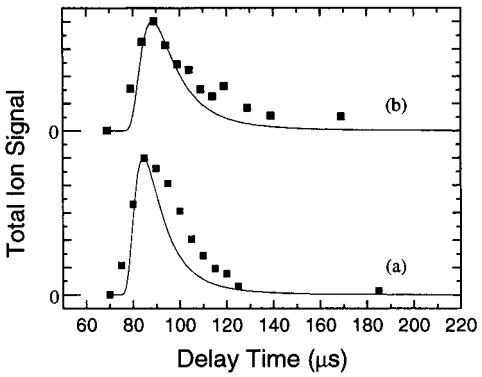

Figure 3. Comparison of the total ion signal from ethylene glycol particles with the predicted gas arrival time distributions based on a three-dimensional Maxwell−Boltzmann distribution of gas velocities. The two distributions have been normalized to the same area. The heater temperature and heater − ionization region distance is 500 K and 8.0 mm for spectrum a and 550 K and 10.5 mm for spectrum b. Time zero is when the particle passes through the center of the ionization region on its way to the heater.

from ionization of the background gas. It is possible that particles not detected by the diode lasers hit the heater, are vaporized, and thus generate a large background gas pressure, which is then ionized whenever the laser is fired. To establish that these spectra result from a single aerosol particle, we examined the total ion signal from ethylene glycol particles (2−4 μm) as a function of the VUV laser delay time with a heater temperature of 500 K. Ion signals resulting from background vapor ionization would be independent of the laser delay, while single particles would produce a pulse of gas that creates a transient locally high pressure. The result of this measurement is plotted in Figure 3a. Time zero in this figure is the time at which the particle passes through the ionization region on its way to the heater. The laser delay thus represents the time required for the particle to travel the few millimeters from the ionization region to the heater plus the time required for the vapor to return to the ionization region. The resulting total ion signal rises from near zero at short delay times to a maximum at a delay of 85 μs and then decreases as the vapor expands into the vacuum chamber and is pumped away. The pumping speed is clearly sufficient to remove the vapor before the next particle arrives, ~0.1 s later.

The delay and shape of the profile in Figure 3a can be related quantitatively to the particle velocity and the Maxwell−Boltzmann distribution of speeds generated by the heater vaporization process. The average velocity of these particles prior to evaporation was determined to be 120 m/s from the light scattering of the two green diode lasers. At the heater surface, the particle is converted into a vapor plume that leaves the heater with some velocity distribution, which we can approximate with a Maxwell−Boltzmann distribution given by eq 1, where M is the molecular

$$F(v)\,\mathrm{d}v = 4\pi\left(\frac{M}{2\pi RT}\right)^{3/2} v^2 \exp\left(\frac{Mv^2}{2RT}\right)\mathrm{d}v \qquad (1)$$

weight of the ethylene glycol, R is the gas constant, and T the temperature (in K). The mean speed of the gaseous ethylene glycol molecules at a temperature of 500 K is 448 m/s. From this information, we can determine the distance, D, between the laser interaction region and the heater by equating the mean delay time of 85 μs with the following sum: $D/120 + D/448$. This yields a distance of 8.0 mm, which is close to our estimated distance determined by viewing the heater through the view port.

We can convert the Maxwell−Boltzmann distribution in eq 1 into a distribution of molecule arrival times at the laser interaction region, which can be compared to the experimentally observed arrival time distribution. Equation 1 can be transformed into an arrival time distribution by substitution of D/t for the velocity v and converting the differential, $\mathrm{d}v = -Dt^{-2}\,\mathrm{d}t$. This arrival time distribution is given by

$$f(t) = 4\pi\left[\frac{M}{2\pi RT}\right]^{3/2}\frac{D^3}{t^4}\exp\left[\frac{-MD^2}{2RTt^2}\right] \qquad (2)$$

where t is the time required for the gaseous molecule to travel distance D from the heater to the ionization region. Because the distance from the heater to the VUV laser (8.0 mm) and the distance over which we ionize and extract our vapor molecules (~1 cm) define a small angle relative to the heater surface normal (0.56 rad), the angular distribution of molecules within the plume has little effect on $f(t)$. For example, calculations assuming a cosine distribution only produced deviations of roughly 6%. However, this cosine dependence would need to be considered for decreased heater distances, D.

This normalized function was compared to the normalized signal generated from the ethylene glycol particles. The experiment was repeated at several temperatures and heater distances. Figure 3 compares the results for the 8.0-mm distance at 500 K (a) and for a 10.5-mm distance at 550 K (b). The Maxwell−Boltzmann distribution profiles in Figure 3 were shifted to larger times to account for the flight of the particle from the ionization region to the heater and subsequent vapor formation at the heater surface. The shapes of the profiles match reasonably well with the predicted arrival distribution predicted by eq 2. The difference between the two distributions is due primarily to the different heater distances. The larger heater distance results in a broader arrival time distribution and, therefore, a lower peak intensity. The temperature variation (500 vs 550 K) is too small to result in a noticeable change in the distribution. The range of temperatures that gave a good signal was in fact quite limited (~500−600 K) so that we could not investigate the temperature dependence of the arrival time distribution. Although the calculated and experimental gas arrival time distributions are not identical, their approximate agreement indicates that modeling the vaporization with a three-dimensional Maxwell−Boltzmann distribution seems to be reasonable for single-component particles.

However, the analysis of multicomponent particles may be more complex. First it is possible that the more volatile components may evaporate more quickly, although we do not know how big a difference this would make. Of more concern is the different speeds at which molecules of different molecular weights will be ejected toward the photoionization region. For instance, oleic acid with its molecular weight of 282 amu would require 38 μs, while the ethylene glycol (MW = 62) requires only 18 μs to travel the 8-mm distance between the heater and the VUV laser. This difference of 20 μs essentially encompasses the full width at half-maximum of the arrival time distribution in Figure 3. This disparity

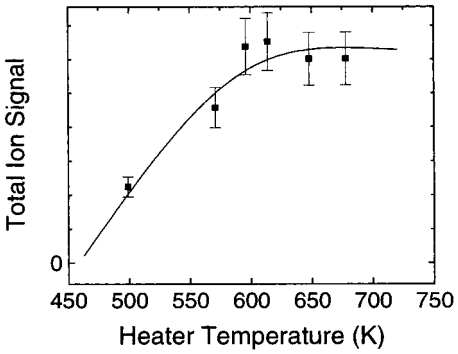

Figure 4. Total ion signal for oleic acid particles as a function of the heater temperature. The leveling off at high heater temperatures is evidence for complete vaporization of the entire particle.

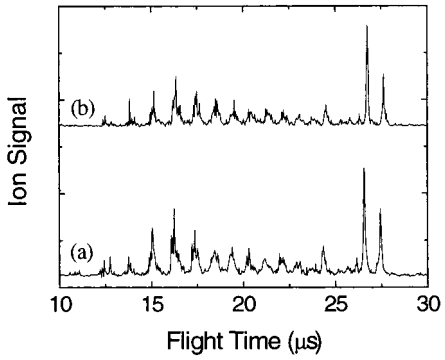

Figure 5. Comparison of oleic acid TOF mass spectra obtained by vaporizing the particles with the heater (a) and the infrared CO_2 laser (b). Note the similarity in the resulting mass spectra. Each spectrum is the average of 100 single-particle mass spectra.

can be reduced by decreasing the heater to photoionization distance. In addition, an effect that may mitigate this problem is the nature of the gas expansion. If the molecules upon evaporation experience a large number of collisions, the disparity between the velocities of the heavy and light molecules will be reduced.

Vaporization Temperature Effects. Figure 2 shows three TOF mass spectra of oleic acid particles resulting from thermal heating at different temperatures: 500, 570, and 650 K. It is evident that the total ion signal increases with increasing temperature because a greater portion of the particle evaporates.

Figure 4 displays the total ion signal generated from oleic acid particles as a function of the heater temperature. The total ion signal levels off above 600 K and even seems to decrease slightly. We attribute the leveling off to the onset of complete vaporization of the particle above 600 K. The drop in signal above this temperature may be due to the lower gas density as the temperature is increased. The Maxwell−Boltzmann distribution broadens out as the temperature is increased so that gas density some 8 mm from the source is reduced correspondingly. The reduction in the maximum in this distribution between 600 and 700 K is ∼10%, which is close to the observed reduction.

The distance of the heater from the ionization region was made sufficiently large to prevent distortion of the electric field used to extract the ions from the source. However, at this large distance (∼8 mm), the laser intersects only a small fraction of the gas molecules because the plume is spread over a considerable volume. Although the gas plume is spreading in three dimensions, the VUV laser ionizes along the whole axis of the laser beam, so that we lose gas density in only two dimensions. We thus expect that a reduction in the heater distance will increase the signal by approximately the square of that distance. A smaller diameter heater is currently being designed so that it can be inserted to within a few millimeters of the ionization region without distortion of the electric field.

The oleic acid mass spectra in Figure 2 show that the degree of fragment ion production is strongly temperature dependent. At the lowest temperatures, the mass spectrum is composed primarily of the molecular ion (M^+) and its H_2O loss fragment. However, as the heater temperature is increased, fragmentation becomes more prominent while the parent ion peak diminishes. This increased fragmentation is due to the increased internal energy of the vaporized oleic acid molecules, which results in fragment ions once the molecule is ionized by the VUV laser. The observation of a strong parent ion peak upon VUV photoionization is in stark contrast to the EI ionization mass spectrum of oleic acid in which the parent ion peak is nearly absent.[17]

The ability to manipulate the fragmentation pattern by adjusting the heater temperature provides some flexibility in the mass spectral analysis. At lower heater temperatures, less complicated mass spectra are generated. This situation is desirable in the analysis of multicomponent particles. Although the entire particle may not be vaporized at these low temperatures, the dominant presence of the parent ions will aid in the identification of the various molecular components in the particles. On the other hand, if fragmentation trends are important for identifying a compound, higher energy mass spectra can be generated by simply elevating the vaporization temperature. Likewise, if quantitative studies are important, the temperature can be raised to ensure that the entire particle is vaporized.

Comparison of Thermal Vaporization and Laser Desorption. Mass spectra of oleic acid particles (2−4 μm) were collected at several CO_2 laser powers and heater temperatures to compare laser desorption with the thermal vaporization method. Figure 5 shows TOF mass spectra resulting from the thermal vaporization/laser ionization and the two-step laser desorption/ionization of oleic acid. A heater temperature of 650 K and a CO_2 laser power of 88 mJ/pulse were used for the spectra in Figures 5a and b, respectively. Spectral features for the parent ion (M^+) and the water loss ion $(M-H_2O)^+$ are prominent in both spectra. In addition, the relative intensities of the parent and the various fragment ion peaks are remarkably similar for the two modes of vaporization. This demonstrates that the internal energy distribution created by the CO_2 laser and the heater are very similar, a trend that was observed for several heater temperatures and CO_2 laser powers.

Comparing the signal levels obtained with the CO_2 laser and the heater reveals the relative sensitivities or efficiencies of these two methods. At high CO_2 laser powers, the vaporization occurs within 1 μs. If the VUV ionization laser is fired within 2 μs, then all molecules with speeds less than 500 m/s travel less than 1 mm and can be ionized. That is, the vapor plume is very dense

(17) Stein, S. E. In *NIST Chemistry WebBook, NIST Standard Reference Database Number 69*; Mallard, W. G., Linstrom, P. J., Eds.; National Institute of Standards and Technology (http://webbook.nist.gov): Gathersburg, MD, 2001.

(although 10^9 times less dense than the condensed-phase particle) so that most of the molecules can be intercepted by the VUV laser. Under these conditions, the signal levels are much higher than those obtained from the heater. However, at lower CO_2 laser power where the vaporization process is much slower, the optimum VUV laser delay is larger and the signals are correspondingly smaller. Under these conditions, the ion signals obtained from the CO_2 laser vaporization and the heater vaporization are approximately the same.

The particle hit rates, defined as the fraction of timed particles that are ionized and detected, for the two methods were also compared. The ability to record mass spectra from nearly all particles that are detected by the timing diode lasers is an important issue when aerosols are sampled in real time. With the two-laser method, our particle hit rates are between 90 and 100%. For the thermal vaporization studies, the hit rate was even higher, between 98 and 100%. The slight improvement in the ability to successfully ionize each timed particle is a result of the much less stringent timing requirements when only one laser is used. The high efficiency associated with the thermal vaporization method is another indication of the effectiveness of this technique.

The sensitivity associated with this technique is already efficient for laboratory characterizations of aerosol particles. Based on the current design, single-component particles on the order of 1 μm should be detectable. However, the analysis of multicomponent atmospheric particles will require much greater sensitivity than currently exists. To improve the sensitivity of this method, several changes in instrumental design are being explored. As previously described, the use of a smaller diameter heater will allow for more efficient analysis. By the use of a smaller diameter heater (and possibly guard electrodes), we can minimize the field distortion, allowing the heater to be placed closer to the VUV laser. This reduced distance from the laser to the heater should increase our signal by a factor of r_{old}^2/r_{new}^2, where r_{new} and r_{old} correspond to the proposed and current distances between the heater and the ionization region. For example, moving the heater from 8 mm to 2 mm from the VUV laser would increase the signal by a factor of 16. Also, increasing the fluence associated with the VUV laser should enhance our overall signal. Ultimately, we hope to improve the sensitivity of this method, allowing for sampling of atmospheric aerosols.

CONCLUSIONS

The combination of thermal vaporization with VUV ionization provides a viable alternative to two-step laser desorption/ionization. This method allows for the generation of single-particle mass spectra comparable to those of the two-step laser desorption/ionization. The temperature of the heater can be adjusted to control the amount of vaporization, as well as the extent of fragmentation. An improved version of this apparatus, with a smaller heating surface placed within 2 mm of the ionization region should increase the signal level by a factor of 16. Future studies will evaluate the effectiveness of this technique for inorganic constituents, as well as complex mixtures.

Received for review November 29, 2001. Accepted February 5, 2002.

AC011225A